NASA Contractor Report 185179

An Improved Algorithm for the Modeling of Vapor Flow in Heat Pipes

Leonard K. Tower and Donald C. Hainley

Sverdrup Technology, Inc.
NASA Lewis Research Center Group
Cleveland, Ohio

December 1989

Prepared for
Lewis Research Center
Under Contract NAS3-25266

National Aeronautics and
Space Administration

AN IMPROVED ALGORITHM FOR THE MODELING OF VAPOR FLOW IN HEAT PIPES

Leonard K. Tower and Donald C. Hainley
Sverdrup Technology, Inc.
NASA Lewis Research Center Group
Cleveland, Ohio 44135

INTRODUCTION

The NASA Lewis Research Center has developed a steady state heat pipe code for use in heat pipe design and analysis of laboratory data, suitable for microcomputers as well as larger machines.[1] It has become apparent that the vapor flow algorithms in this and similar codes[2,3] are not very satisfactory at conditions where compressibility is important. Heat pipes having axially varying heat input, sequential evaporators, or operating near the sonic limit, are not handled well in these codes. Typical of the problems in some codes is the prediction of a negative absolute pressure within an evaporator with large heat input, because of improper treatment of compressibility effects. The ability to handle compressibility and variable heat input is desired for the NASA Lewis code. Therefore, an accurate vapor flow algorithm concise enough to operate on a microcomputer at a reasonable speed and incorporating these features was sought. Finite difference techniques which have been used effectively in fundamental studies of heat pipe vapor dynamics[4,5] were precluded by code size. Among sources consulted in an attack on this problem was the book by Ivanovskii et al.[6] which reviews several studies leading to one-dimensional algorithms for compressible vapor flow in heat pipes.

For the present work, Busse's[7] paper on pressure drop in the vapor phase was used as a starting point. His equations for incompressible flow were readily rederived to include change in density. In addition, the usual assumption of a saturation temperature across each section of the pipe, determined by the local static pressure, was eliminated. In view of the studies of DeMichele,[4] a mean vapor temperature differing from the wall temperature was found from a boundary-layer-type energy equation. The resulting equations were derived so as to be suitable for liquid metal working fluids having two vapor species as well as for fluids with a single vapor species. The algorithm is intended only for the evaporator and adiabatic sections of the heat pipe, because vapor flow in the condenser is complicated by the onset of turbulence and reverse flow.

ANALYSIS

In the analysis to follow, the appropriate features of Busse's[7] method will be introduced, and the development will proceed from there. In addition, some major assumptions for the heat pipe sections being considered should be indicated at the outset: Flow is laminar. The ideal gas law applies to components of the vapor. The equations allow for local chemical equilibrium among species in the vapor. Phase equilibrium occurs only at the wall, so liquid droplets are absent in the vapor. Following Busse,[7] no tangential velocity component exists at the wall in mass addition or removal, the radial pressure gradient may be neglected, and the velocity components are zero at the closed ends of the heat pipe. Also, his method of imposing a negligible radial pressure gradient by equating the mean axial pressure gradient over the cross section to the axial pressure gradient along the center line was used.

Busse[7] began with the axial axisymmetric Navier-Stokes equation

$$\frac{\partial p}{\partial z} = -\rho\left(u\,\frac{\partial v}{\partial r} + v\,\frac{\partial v}{\partial z}\right) - \frac{\eta}{r}\frac{\partial}{\partial r}\,r\left(\frac{\partial u}{\partial z} - \frac{\partial v}{\partial r}\right) \tag{1}$$

where p is pressure, r is radial distance, u is radial velocity, v is axial velocity, z is axial distance, η is dynamic viscosity, and ρ is density. Busse integrated the mass conservation equation with respect to u so that this term can be eliminated. This is also done in the present analysis except that density is variable in z and r:

$$u = -\frac{1}{r\rho}\int_0^r \frac{\partial}{\partial z}\,(\rho v)r'\,dr' \tag{2}$$

When equation (2) is combined with equation (1) the following results:

$$\frac{\partial p}{\partial z} = \frac{1}{r}\left[\frac{\partial v}{\partial r}\left(\int_0^r \rho\,\frac{\partial v}{\partial z}\,r'\,dr' + \int_0^r v\,\frac{\partial \rho}{\partial z}\,r'\,dr'\right)\right] - \rho v\,\frac{\partial v}{\partial z} + \frac{\eta}{r}\frac{\partial}{\partial r}\,r\,\frac{\partial v}{\partial r} \tag{3}$$

Here, the axial variation of u has been neglected in the viscous term. The assumption is made that the radial variation of density is much less than the radial variation of the axial velocity since the latter vanishes at the wall. On the basis of this assumption, a presently undefined mean density ρ_m and its axial derivative are extracted from the integrals, yielding

$$\frac{\partial p}{\partial z} = \frac{1}{r}\left[\frac{\partial v}{\partial r}\left(\rho_m\int_0^r \frac{\partial v}{\partial z}\,r'\,dr' + \frac{\partial \rho_m}{\partial z}\int_0^r vr'\,dr'\right)\right] - \rho v\,\frac{\partial v}{\partial z} + \frac{\eta}{r}\frac{\partial}{\partial r}\,r\,\frac{\partial v}{\partial r} \tag{4}$$

The crux of Busse's attack on the incompressible case is the assumption of an approximate velocity profile which satisfies all the boundary conditions. It incorporates a parameter $A(z)$ which may be constant or may vary with position, depending on mass influx boundary conditions. The same profile will be employed in this analysis:

$$v = 2v_m\left(1 - \frac{r^2}{R^2}\right)\left[1 + A(z)\left(\frac{r^2}{R^2} - \frac{1}{3}\right)\right] \tag{5}$$

Here, v_m is the mean axial velocity and R is the vapor space diameter. When $A(z) = 0$, equation (5) reduces to the Poiseuille profile. Integration of equation (4) over the cross section of the pipe and manipulation give

$$\frac{dp_m}{dz} = -\frac{4}{3}\frac{d}{dz}\left[\left(1 - \frac{A}{6} + \frac{2A^2}{45}\right)\left(v_m^2\rho_m\right)\right] - \frac{8\eta v_m}{R^2}\left(1 + \frac{2A}{3}\right) \tag{6}$$

The mean density is assumed to be related to the pressure and a mean temperature T_m by the ideal gas law, which yields upon differentiation

$$\frac{d\rho_m}{dz} = (GRP)\frac{d\ \ell n\ p}{dz} - (GRP)\frac{d\ \ell n\ T_m}{dz} \tag{7}$$

where

$$GRP = 1 - \frac{\partial\ \ell n\ R_g}{\partial\ \ell n\ p} \quad \text{and} \quad GRT = 1 + \frac{\partial\ \ell n\ R_g}{\partial\ \ell n\ T_m}$$

and where R_g, the gas constant, may depend on pressure and temperature if chemical reactions are considered.

Continuity requires that the vapor mass flux $m(z)$ at any cross section equals the product of mean density ρ_m, the vapor cross-sectional area A_v, and the mean axial velocity $v_m(z)$. From this relationship and equation (7) the axial derivative of v_m is found to be:

$$\frac{d\ \ell n\ V_m}{dz} = \frac{d\ \ell n\ m}{dz} - \frac{d\ \ell n\ A_v}{dz} - (GRP)\frac{d\ \ell n\ p}{dz} + (GRT)\frac{d\ \ell n\ T_m}{dz} \tag{8}$$

Equations (6) to (8) are combined and the indicated integrations are performed. Dropping the distinction between the mean cross section pressure and the local pressure by Busse's approximation gives

$$\left[1 - \frac{4\rho_m v_m^2}{3p}(GB)(GRP)\right]\frac{d\ \ell n\ p}{dz} + \left[\frac{4\rho_m v_m^2}{3p}(GB)(GRT)\right]\frac{d\ \ell n\ T_m}{dz} - \frac{4\rho_m v_m^2}{3}(HB)\frac{dA}{dz}$$

$$= -\frac{8\eta v_m}{R^2 p}\left(1 + \frac{2A}{3}\right) - \frac{8\rho_m v_m^2}{3p}(GB)\left(\frac{d\ \ell n\ m}{dz} - \frac{d\ \ell n\ A_v}{dz}\right) \tag{9}$$

where

$$GB = \left(1 - \frac{A}{6} + \frac{2A^2}{45}\right) \quad \text{and} \quad HB = -\left(1 - \frac{8A/15}{6}\right)$$

The variation of A_v with z is understood to be small.

The mean temperature T_m is evaluated by means of an energy integral. Figure 1 shows the control volume through which energy is transported. The energy flows into the boundary are equated with the energy flows out, internal energy and pressure are eliminated by using enthalpy, and the limit $\Delta z \to 0$ is taken, to give

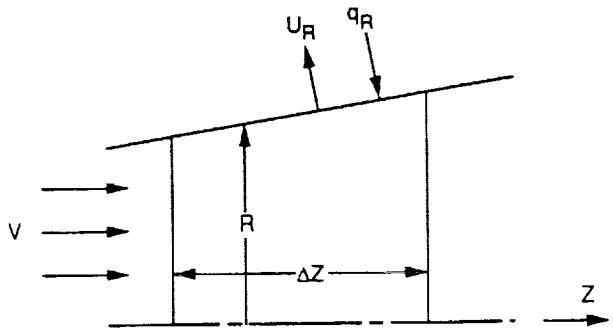

Figure 1. – Control volume for the integral energy equation.

$$\int_0^R \left[\frac{d}{dz}\,\rho v\left(h + \frac{v^2}{2}\right)\right] r\,dr = \int_0^R \Phi r\,dr + q_R\,R - \rho R u_R \tag{10}$$

where h is the enthalpy of the mixture per unit mass, q_R is the energy flux entering from the wall of the pipe, and Φ is the viscous dissipation per unit volume. The relation for u_R, the wall radial velocity, is given by the mass conservation equation in the form

$$u_R = -\frac{1}{R\rho_R}\int_0^R \frac{d}{dz}\,(\rho v) r\,dr \tag{11}$$

The energy influx q_R is specified as $-\rho_R u_R(e_R + u_R^2/2)$, where e_R is internal energy. The result of combining equations (10) and (11) is

$$\int_0^R \left(h + \frac{v^2}{2} - H_R\right)\frac{d}{dz}\,(\rho v) r\,dr + \int_0^R \rho v\,\frac{dh}{dz}\,r\,dr + \int_0^R \rho v^2\,\frac{dv}{dz}\,r\,dr = \int_0^R \Phi r\,dr \tag{12}$$

The mean value of both the enthalpy and the density can be separately extracted from the integrals if the assumption is again made that the variation of both variables with radius is much less than that of axial velocity. When these mean values have been extracted, and terms common to all expressions cancelled, the energy equation becomes

$$\left(h_m - H_R\right)\frac{d}{dz}\,\rho_m v_m + \frac{1}{R^2}\left(\int_0^R v^3 r\,dr\right)\frac{d\rho_m}{dz} + \rho_m v_m\,\frac{dh_m}{dz} + \frac{\rho_m}{R^2}\int_0^R \frac{dv^3}{dz}\,r\,dr = \frac{2}{R^2}\int_0^R \Phi r\,dr \tag{13}$$

where

$$H_R = h_R + \frac{u_R^2}{2}$$

If chemical equilibrium in the vapor must be considered, enthalpy h_m becomes a function of both T_m and p. When its derivative is inserted into equation (13) with equations (7) and (9), and the integrations are performed, the result is

$$\left[\left(\frac{\partial h_m}{\partial \ln p}\right)_{T_m} - F_3(GRP)\right]\frac{d \ln p}{dz} + \left[\left(\frac{\partial h_m}{\partial \ln T_m}\right)_p + F_3(GRT)\right]\frac{d \ln T_m}{dz} + (HAF)\frac{dA}{dz}$$

$$= 8\eta\left[\frac{(1 + 2A^2/9)v_m}{\rho_m R^2}\right] - (HVE)\left(\frac{d \ln m}{dz} - \frac{d \ln A_v}{dz}\right) \qquad (14)$$

where

$$F_3 = 8\left(\frac{1}{4} - \frac{A}{10} + \frac{A^2}{30} - \frac{2A^3}{945}\right)$$

$$HAF = -\frac{2}{5}\left(1 - \frac{2A}{3} + \frac{4A^2}{63}\right)$$

$$HVE = h_m - H_R + \left(\frac{3F_3 v_m^3}{2}\right)$$

An additional equation required to find the three dependent variables p, A, and T_m comes from Busse's[7] approximation that the axial gradient of the mean pressure equals the center line pressure gradient. The latter, from equation (1) for $r = 0$ using equations (4) and (5), is

$$\left[1 - \frac{4\rho_m v_m^2}{p}(1 - A/3)^2(GRP)\right]\frac{d \ln p}{dz} + \left[\frac{4\rho_m v_m^2}{p}(1 - A/3)^2(GRT)\right]\frac{d \ln T_m}{dz}$$

$$- \left[\frac{4\rho_m v_m^2}{3p}(1 - A/3)\right]\frac{dA}{dz} = \frac{-8\eta v_m}{pR^2}(1 - 4A/3)$$

$$- \left[\frac{4\rho_m v_m^2}{p}(1 - A/3)^2\right]\left(\frac{d \ln m}{dz} - \frac{d \ln A_v}{dz}\right) \qquad (15)$$

The mass flux is related to the heat flux into the pipe by

$$\frac{dq_R}{dz} = \frac{1}{2\pi R}\frac{dm}{dz}\left[h_{v\ell} + \left(\frac{1}{2\pi R\rho_R}\frac{dm}{dz}\right)^2\right] \qquad (16)$$

where the kinetic energy of the injected vapor has been incorporated, and $h_{v\ell}$ is the heat of evaporation. Equations (9), (14), and (15), with equation (16) and appropriate boundary conditions enable a solution for p, A, and T_m.

The equations derived here pertain to alkali metal working fluids if equilibrium between monomeric and dimeric species is experienced. With proper application, they also apply to working fluids of a single gaseous species. If, in the case of the alkali metals, composition remains fixed from the point of injection, the equations must be modified. This case has been considered but the results are much less satisfactory than for equilibrium and are not presented here.

RESULTS AND DISCUSSION

To illustrate the application of the algorithm, several cases were run involving alkali liquid metal working fluids. Entropies and enthalpies of the species referred to a common base that includes chemical energy were used with polynomials for the specific heats to find thermodynamic properties.[8] These data enabled the determination of vapor pressure, heat of vaporization, various first derivatives and composition of the vapor phase. The latter includes both monomers (atoms) and dimers (molecules) in the case of alkali metals. The assumption is made that the ideal gas law applies to each of the vapor species. While it would be desirable to incorporate real gas effects in the form of virial equations, this would greatly complicate the computations.

The three equations involving the first derivatives of p, A, and T_m were solved by a simple Runge-Kutta routine[9] for the set of simultaneous equations (9), (14), and (15). No study of the effect of step size on the precision of results was made. Each computation began with 20 uniform steps in the evaporator, but step size was reduced as the slope of p became increasingly steep in the vicinity of the sonic limit.

Figure 2 illustrates a simple application of the algorithm which solves the equation set. The heat input to a sodium-filled heat pipe of 0.02 m diameter with an evaporator length of 0.1 m was increased until the pipe was choked at an evaporator endcap vapor temperature of 900 K and a heat input of 5870 W. The sonic limit computed from the approximation of Busse[10] was about 5580 W. Figure 2 shows the profiles of vapor mean temperature T_m, wall temperature T_R, the velocity profile parameter A, and the pressure ratio p/p_0 through the evaporator, where subscript 0 denotes the vapor condition at $z = 0$, the endcap. Figure 3 shows the velocity profile v/v_m at the downstream end of the evaporator where choking occurs, with a Poiseuille profile for comparison. The maximum value did not occur at the centerline, as expected. Busse's approximate profile is a three-point fit, so the profile shown in Figure 3 must be regarded as the best representation of a very flat profile available under the circumstances.

In the next example two evaporator sections in sequence were considered, the first 0.2 m long, the second 0.1 m long, separated by an adiabatic section of 0.2 m length. The working fluid was sodium and the evaporator end cap temperature was 1000 K. Both evaporator sections were receiving heat at the rate of 71 600 W/m, which resulted in choke at the end of the second evaporator. Figure 4 shows the profiles of temperature, pressure ratio, and A. The scale of the figure is too small to show clearly the decline in the parameter A in the adiabatic section from 0.738 to 0.704. In incompressible flow, the limit for A in very long adiabatic sections should decline toward zero, the Poiseuille condition.

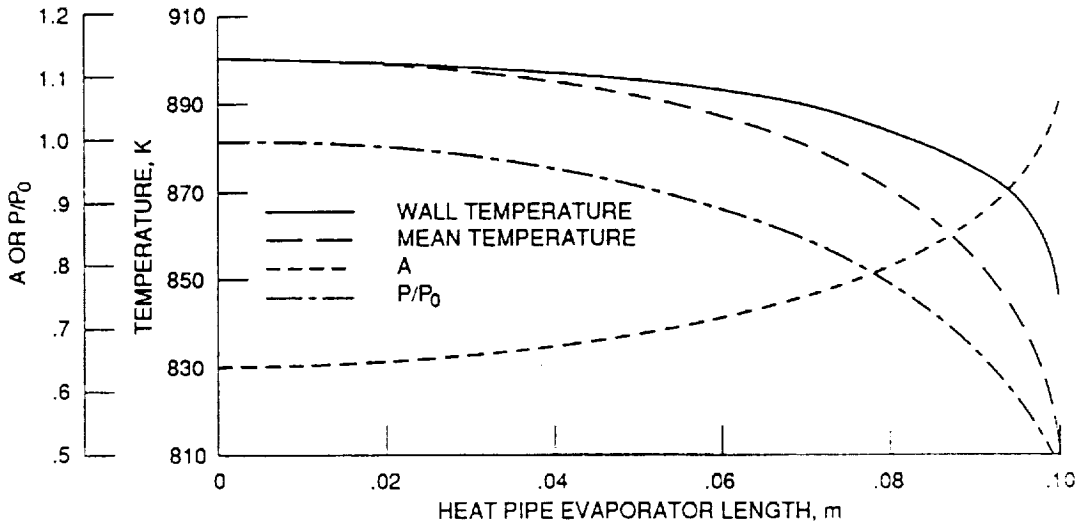

Figure 2. – Variation of heat pipe parameters with location.

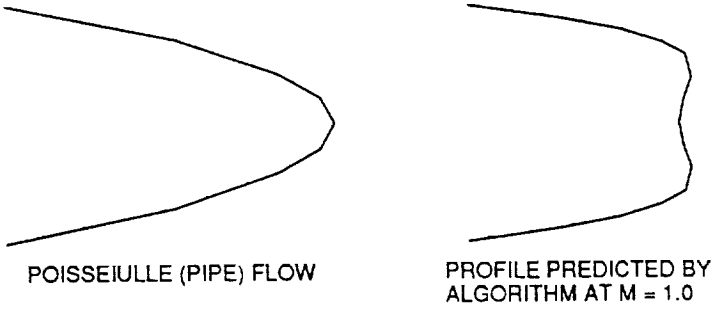

Figure 3. – Comparison of V/V_m for Poisseiulle and chocked flow conditions.

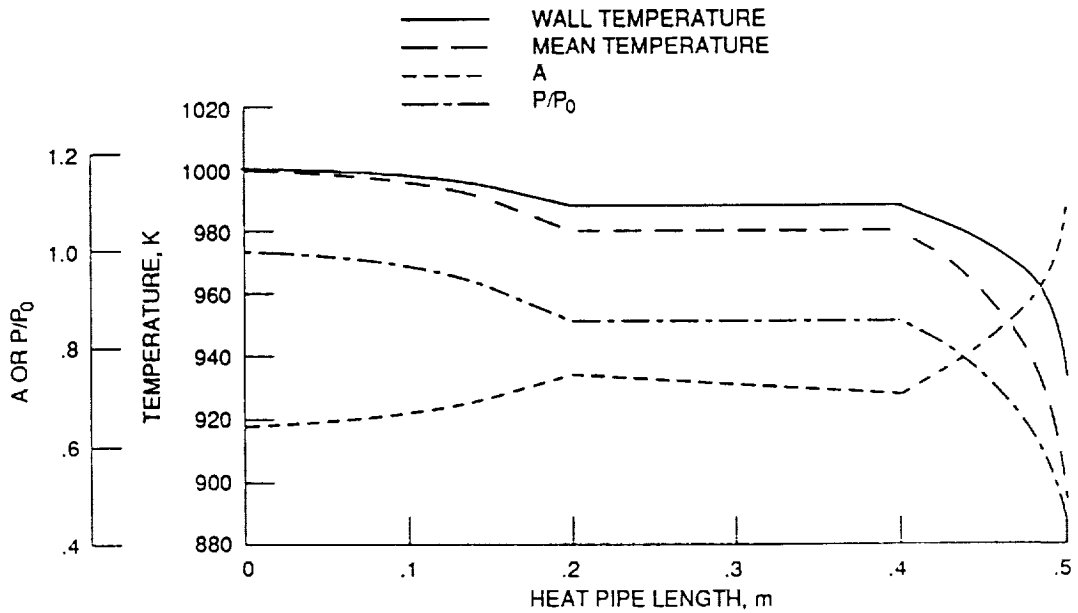

Figure 4. – Variation of heat pipe parameters with location for a multi–location heat source on evaporator.

Another example shows the sonic limit heat transport against evaporator endcap temperature for a sodium-filled evaporator of 0.02 m diameter and 0.1 m length. The short evaporator length minimized the viscous pressure loss, so the results can be compared to those computed from inviscid equations of Busse[10] and Levy.[11] A simple control structure appended to the vapor pressure subroutine generated figure 5 in a short time.

The most suitable data against which to check the algorithm are those of Ivanovskii et al.[6] They inserted a temperature microprobe into a sodium heat pipe having an evaporator length of 0.1 m, an adiabatic section length of 0.05 m, a condenser length of 0.55 m, and a diameter of 0.014 m. Temperatures were read at intervals along the axis with the probe. Liquid-saturated wicking on the probe was to ensure that the temperatures being observed were the same as those at the vapor-liquid interface. No details were given concerning any effect of the pressure field around the probe tip on the measured temperature. For an input of about 500 W, stated to be accurate to within 6 to 10 percent, the data are shown in figure 6. Also shown are lines of T_m and T_R computed by the algorithm. Equations (9), (14), and (15) were used only in the evaporator and adiabatic sections. An extension into the condenser was made by equating T_m to T_R beyond the point where T_m exceeded T_R. The justification is the observation that at some point in the condenser, T_m must converge to T_R as it did at the beginning of the evaporator. For this portion of the solution, the equations were suitably modified to yield as dependent variables only p and A. This simple procedure, enabling the solution to be continued into the condenser, neglected the known complications of condensation shocks and recirculation.

For the same heat pipe at a heat input of 1000 W, figure 7 shows experimental data of Ivanovskii and lines of T_m and T_R from the algorithm. Also shown is a curve of T_R computed by Chen and Faghri[12] using the Phoenics code. It is in basic agreement with the results computed by the algorithm presented here. The Phoenics code, a sophisticated finite difference procedure, can handle far more complex situations than the elementary algorithm herein. These include evaporators with very small ratios of length to diameter and heat pipes of complex cross section. The size of computer required for the Phoenics code and its cost make it less suitable for everyday heat pipe analysis. Furthermore, the simple

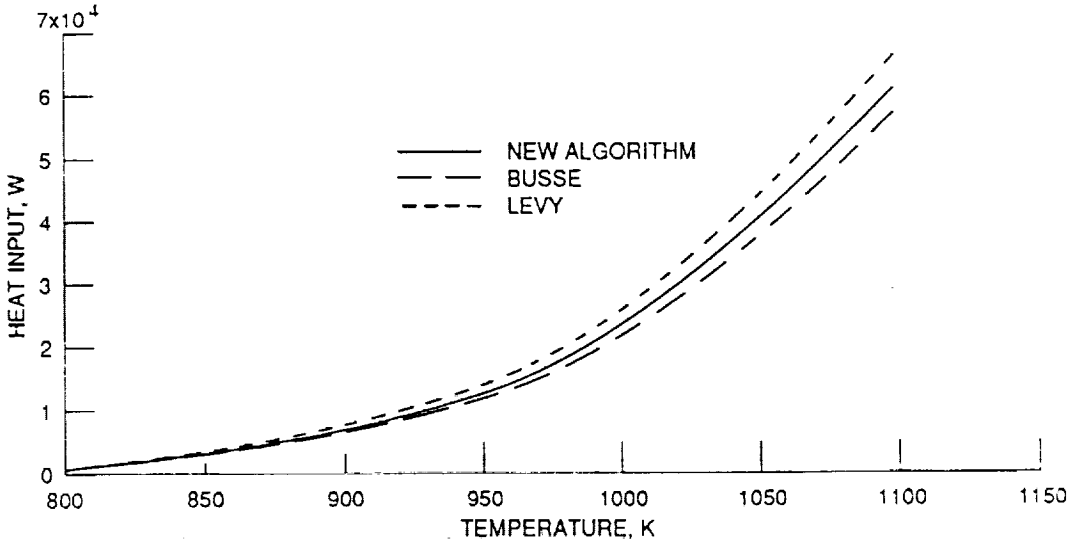

Figure 5. – Sonic limit determination.

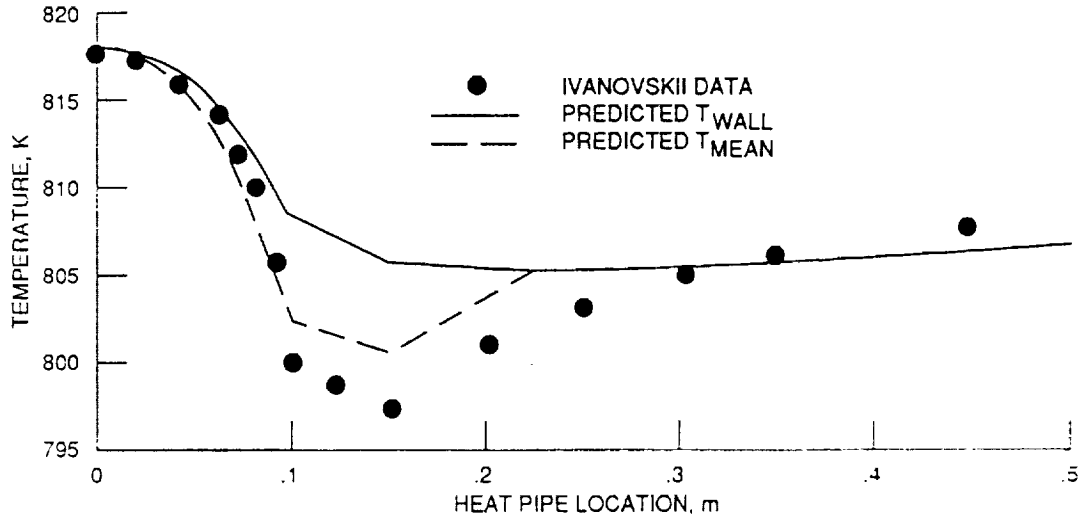

Figure 6. – Comparison of predicted values with Ivanovskii data.

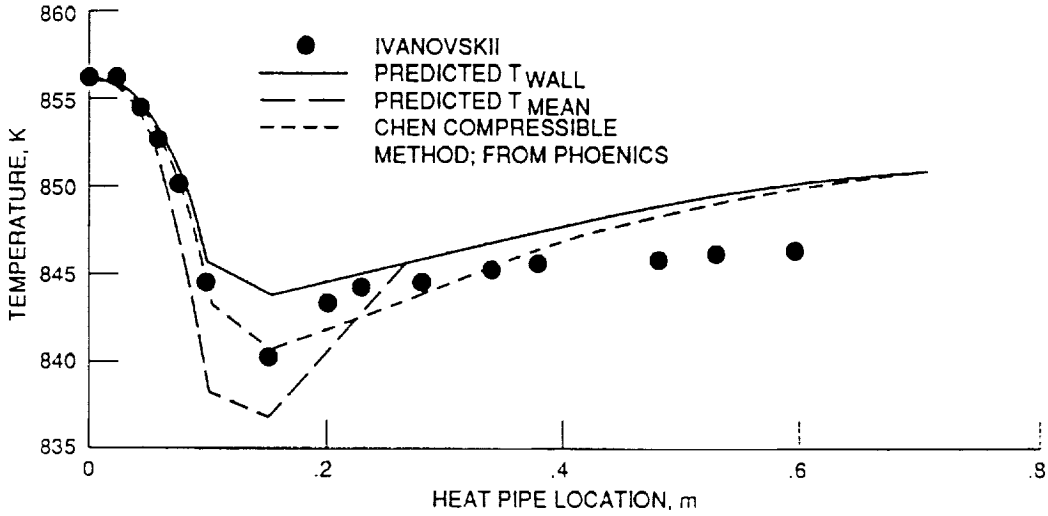

Figure 7. – Comparison of predicted values with Ivanovskii data and results of other methods.

equations derived from first principles in the present paper may facilitate a better physical understanding of the governing phenomena.

CONCLUDING REMARKS

The heat pipe vapor flow algorithm discussed herein has been shown to model the compressible vapor dynamics in the evaporator and adiabatic sections of pipes of conventional proportions. The model has introduced complexities which have usually been ignored. These include chemical equilibrium in the case of liquid metals, a velocity profile parameter dependent upon pressure and temperature, and a mean vapor temperature differing from the vapor interface temperature. Future work might be expended profitably on the introduction of a reasonable temperature profile into the energy equation, and the inclusion of droplet nucleation rates into the momentum and energy equations. Also, a satisfactory representation of the vapor effects in the condenser requires that the transition to turbulence, the treatment of condensation shocks, flow

recirculation, and other phenomena be modeled concisely for use in simple programs on small computers.

REFERENCES

1. Baker, K.W., and Tower, L.K., The Lewis Heat Pipe Code with Application to SP-100 GES Heat Pipes, Trans. 5th Symp. Space Nucl. Power Syst., Albuquerque, NM, Jan. 11-14, pp. 99-103, 1988.

2. Woloshun, K. and Merrigan, M., HTPIPE: A Steady State Heat Analysis Program, Trans. 5th Symp. Space Nucl. Power Syst., Albuquerque, NM, Jan. 11-14, pp. 105-108, 1988.

3. McLennan, G.A., ANL/HTP: A Computer Code for the Simulation of Heat Pipe Operation, Argonne National Laboratory Report ANL-83-108, Nov. 1983.

4. DeMichele, D.W., A Numerical Solution to Axial Symmetric Compressible Flow with Mass Injection and Its Application to Heat Pipes, Ph. D Thesis, University of Arizona, 1970.

5. Busse, C.A., and Prenger, F.C., Numerical Analysis of the Vapor Flow in Cylindrical Heat Pipes, Proc. 5th Int. Heat Pipe Conf. Part I, pp. 214-219, 1984.

6. Ivanovskii, M.N., Sorokin, V.P., and Yagodkin, I.V., The Physical Principles of Heat Pipes, Clarendon Press, Oxford, 1982.

7. Busse, C.A., Pressure Drop in the Vapor Phase of Long Heat Pipes, Proc. 1967 Thermionic Conversion Specialist Conf., Palo Alto, CA, pp. 391-398, 1987.

8. McBride, B.J. and Gordon, S., FORTRAN 4 Program for Calculation of Thermodynamic Data, NASA TN D-4097, Aug. 1967.

9. White, F.M., Viscous Fluid Flow, McGraw-Hill, New York, 1974.

10. Busse, C.A., Theory of the Ultimate Heat Transfer Limit of Cylindrical Heat Pipes, Int. J. Heat Mass Transfer, vol. 16, pp. 169-186, 1973.

11. Levy, E.K., Effects of Friction on the Sonic Velocity Limit in Sodium Heat Pipes, AIAA Paper 71-407, Apr. 1971.

12. Chen, M-M. and Faghri, A., An Analysis of the Vapor Flow and the Heat Conduction Through the Liquid-Wick and Pipe Wall in a Heat Pipe with Single or Multiple Heat Sources, ASME Paper 89-HT-12, 1989.

NASA
National Aeronautics and Space Administration

Report Documentation Page

1. Report No.	2. Government Accession No.	3. Recipient's Catalog No.
NASA CR-185179		

4. Title and Subtitle	5. Report Date
An Improved Algorithm for the Modeling of Vapor Flow in Heat Pipes	6. Performing Organization Code

7. Author(s)	8. Performing Organization Report No.
Leonard K. Tower and Donald C. Hainley	None (E-5195)
	10. Work Unit No. 586-01-21

9. Performing Organization Name and Address	11. Contract or Grant No.
Sverdrup Technology, Inc. NASA Lewis Research Center Group Cleveland, Ohio 44135	NAS3-25266
	13. Type of Report and Period Covered Contractor Report Final
12. Sponsoring Agency Name and Address	14. Sponsoring Agency Code
National Aeronautics and Space Administration Lewis Research Center Cleveland, Ohio 44135-3191	

15. Supplementary Notes

Project Manager, James Calogeras, Power Technology Division, NASA Lewis Research Center. Prepared for the 7th International Heat Pipe Conference sponsored by the Luikov Heat and Mass Transfer Institute, Minsk, U.S.S.R., May 21-25, 1990.

16. Abstract

This paper presents a heat pipe vapor flow algorithm suitable for use in codes on microcomputers. The incompressible heat pipe vapor flow studies of Busse are extended to incorporate compressibility effects. The Busse velocity profile factor is treated as a function of temperature and pressure. The assumption of a uniform saturated vapor temperature determined by the local pressure at each cross section of the pipe is not made. Instead, a mean vapor temperature, defined by an energy integral, is determined in the course of the solution in addition to the pressure, saturation temperature at the wall, and the Busse velocity profile factor. For alkali metal working fluids, local species equilibrium is assumed. Temperature and pressure profiles are presented for several cases involving sodium heat pipes. An example for a heat pipe with an adiabatic section and two evaporators in sequence illustrates the ability to handle axially varying heat input. A sonic limit plot for a short evaporator falls between curves for the Busse and Levy inviscid sonic limits.

17. Key Words (Suggested by Author(s))	18. Distribution Statement
Heat pipe; Heat pipe computer code; Compressibility; Heat pipe evaporator; Space radiator	Unclassified – Unlimited Subject Category 34

19. Security Classif. (of this report)	20. Security Classif. (of this page)	21. No. of pages	22. Price*
Unclassified	Unclassified		

NASA FORM 1626 OCT 86

*For sale by the National Technical Information Service, Springfield, Virginia 22161